JVI Accepted Manuscript Posted Online 9 October 2019
J. Virol. doi:10.1128/JVI.00663-19

PDZ Domain-Containing Protein NHERF-2 is a Novel Target of Human Papillomavirus type 16 (HPV-16) and HPV-18

Nathaniel Edward Bennett Saidu[1], Vedrana Filić[2], Miranda Thomas[3], Vanessa Sarabia-Vega[3], Anamaria Đukić[1], Frane Miljković[1*], Lawrence Banks[3], Vjekoslav Tomaić[1#]

1 Division of Molecular Medicine, Ruđer Bošković Institute, Bijenička cesta 54, 10000 Zagreb, Croatia

2 Division of Molecular Biology, Ruđer Bošković Institute, Bijenička cesta 54, 10000 Zagreb, Croatia

3 International Centre for Genetic Engineering and Biotechnology, Padriciano 99, I-34149 Trieste, Italy

Running Title: NHERF-2 is a target for HPV-16 and HPV-18

#Corresponding author: Vjekoslav Tomaić, tomaic@irb.hr

*Present address: Frane Miljković, Vienna Biocenter, Dr. Bohr-Gasse 9, 1030 Vienna, Austria

Word count abstract: 193

Word count text: 6394

ABSTRACT

Cancer-causing HPV E6 oncoproteins have a Class I PDZ-binding motif (PBM) on their C-terminus, which plays critical roles that are related to HPV life cycle and HPV-induced malignancies. E6 oncoproteins use these PBMs to interact with, and target for proteasome-mediated degradation, a plethora of cellular substrates that contain PDZ domains and which are involved in the regulation of various cellular pathways. In this study, we show that both HPV-16 and HPV-18 E6 can interact with Na^+/H^+ exchange regulatory factor 2 (NHERF-2), a PDZ domain-containing protein, which among other cellular functions also behaves as a tumor suppressor regulating endothelial proliferation. The interaction between the E6 oncoproteins and NHERF-2 is PBM-dependent and results in proteasome-mediated degradation of NHERF-2. We further confirmed this effect in cells derived from HPV-16 and HPV-18 positive cervical tumors, where we show that NHERF-2 protein turnover is increased in the presence of E6. Finally, our data indicate that E6-mediated NHERF-2 degradation results in p27 downregulation and cyclin D1 upregulation, leading to accelerated cellular proliferation. To our knowledge, this is the first report to demonstrate that E6 oncoproteins can stimulate cell proliferation by indirectly regulating p27 via targeting a PDZ domain-containing protein.

IMPORTANCE

This study links HPV-16 and HPV-18 E6 oncoproteins to the modulation of cellular proliferation. The PDZ domain-containing protein NHERF-2 is a tumor suppressor, shown to regulate endothelial proliferation, and here we demonstrate that NHERF-2 is targeted by HPV E6 for proteasome-mediated degradation. Interestingly, this indirectly affects p27, cyclin D1 and CDK4 protein levels and consequently affects cell proliferation. Hence, this study provides information that will improve our

understanding of the molecular basis for HPV E6 function, and it also highlights the importance of the PDZ domain-containing protein NHERF2 and its tumor suppressive role in regulating cell proliferation.

Keywords: HPV, E6 oncoprotein, cervical cancer, NHERF-2, p27, cyclin D1, cell proliferation

INTRODUCTION

Human papillomaviruses (HPVs) are small DNA tumor viruses shown to be the causative agents of cervical cancer, other anogenital cancers, and a number of head and neck cancers (1) (2) (3). Of these, cervical cancer is the most predominant disease caused by HPVs, with more than 600,000 cancers annually worldwide (4). Approximately fifteen mucosotropic HPV types, which are associated with human malignancies, are referred to as High-risk (HR) types (1). HPV-16 and -18 are the most common HR HPV types and are responsible for approximately 80% of cervical cancers worldwide, while the remaining 20% are caused by the other HR types (5). Numerous studies have shown that the collaborative actions of the two major viral oncoproteins, E6 and E7, are responsible for the development and maintenance of HPV-mediated malignancies (6). These two oncoproteins control various cellular pathways with the aim of maintaining an optimal cellular environment for viral replication. However, in instances where this is perturbed, it can lead to initial changes to the infected cells, which can eventually result in malignant transformation (7). HPV E7 stimulates cell cycle progression by targeting the retinoblastoma tumor suppressor (pRB) and the other two pocket proteins, p107 and 130 (8) (9), while E6 interferes with apoptosis by targeting the tumor suppressor p53 (p53) (10). In

addition to p53 protein regulation, E6 also regulates p53 gene transactivation via abolishing p53 transcriptional transactivation activity (5) (6).

Although E6 targeting of p53 is one of the crucial aspects in HPV-induced malignancies, there are also other important functions of E6 that contribute to malignant progression. One of these is the ability of HR HPV E6 oncoproteins to interact with the so-called PDZ domain-containing proteins. The E6 proteins from all of the HR HPV types contain 4 amino acids on their extreme C-termini that correspond to a Class I (PSD-95/Dlg-1/ZO-1) binding motif (PBM). Conversely, this motif is absent from the E6 proteins of Low-risk (LR) HPV types, which cause benign warts (11). Multiple studies have shown that the PBM plays critical roles in various E6 functions that are related to HPV life cycle and malignant transformation. PBM-PDZ interactions lead to increased proliferation of infected cells and are required for optimal amplification and maintenance of viral episomes (12) (13) (14) (15) (16). These interactions also play important roles in the process of HPV-induced cellular transformation in tissue culture and in transgenic mouse models, where they were shown to be required for E6's ability to induce epithelial tumors in cooperation with E7 (17) (18) (19) (12) (20).

HPV E6 oncoproteins interact with a number of PDZ domain-containing proteins that belong to the membrane-associated guanylate kinase (MAGUK) family; and the most extensively studied interacting partners of E6 include the human homologues of the Drosophila disc large protein (hDlg), Scribble (hScrib) and the membrane-associated guanylate kinase with inverted orientation (MAGI) family protein members (11). MAGUK proteins have multiple PDZ domains and, by forming simultaneous interactions with a number of membrane and cytoplasm-associated cellular proteins, they can serve as scaffolds in forming large complexes. Many of them behave as

tumor suppressors and are also involved in the regulation of cell polarity and cell-cell contacts (21) (22). In addition to the MAGUK family member proteins, some other PDZ domain-containing proteins involved in cellular signaling and trafficking have also been characterized as E6 substrates (22) (23). One example is a member of the Na^+/H^+ Exchange Regulatory Factor (NHERF) protein family, NHERF-1, which is involved in a number of important cellular processes such as signaling and transformation (24). HPV-16 E6 can target NHERF-1 for degradation at the proteasome, leading to the activation of the PI3K/AKT signaling pathway, which is an important factor in carcinogenesis (25).

Another member of the NHERF protein family is NHERF-2, which is involved in the regulation of lamellopodia formation and cell migration, and which interacts with the N-cadherin/β catenin (N-Cad/Cat) complex and the PDGFR in epithelial cells (26). NHERF-2 also acts as a scaffold protein for plasma membrane proteins and members of the ezrin/moesin/radixin family, thereby providing a connection between these proteins and the actin cytoskeleton, and controls their surface expression (27). In addition, more recent studies indicate that NHERF-2 is a negative regulator of endothelial proliferation, which is mediated via the cyclin-dependent kinase inhibitor p27 (28).

The fact that NHERF-2 is a PDZ domain-containing protein and is structurally related to NHERF-1, which was previously characterized as a HR HPV-16 E6 oncoprotein substrate, and that it is involved in the regulation of cellular proliferation, suggested that NHERF-2 might also be a cellular substrate of the HPV-16 E6 oncoprotein. Here, we report not only that NHERF-2 is a cellular target of the HPV-16 E6 oncoprotein, but also that it binds to other HPV E6 proteins via their PBM motifs. We further report that both HPV-16 and HPV-18 E6 target NHERF-2 for proteasome-mediated

degradation. NHERF-2 ablation in the presence of HPV E6 leads to p27 downregulation and, consequently, this results in increased cellular proliferation.

RESULTS

E6 oncoproteins from HPV-16, HPV-18 and HPV-33 interact with NHERF-2.

It is well known that the E6 oncoproteins of cancer-causing types of HPV have PBMs through which they can interact with a panel of PDZ domain-containing proteins to elicit a cellular response (11) (21) (22). One of these PDZ-domain containing proteins is NHERF-1, structurally related to NHERF-2, for which it was previously reported to be bound by HPV-16 E6 and consequently degraded at the proteasome (25). We therefore, firstly, wanted to investigate whether the PDZ domain-containing NHERF-2 protein could complex with HPV E6 oncoproteins *in vitro*. A series of GST pulldown assays were performed, where *in vitro* translated NHERF-2 was incubated with GST-16 E6, GST-18 E6, GST-33 E6, GST-18 E6ΔPBM, or GST alone for control. The results in Figure 1A show that HPV-16 E6, HPV-18 E6 and HPV-33 E6 all bind to NHERF-2 and the HPV-16 E6 interaction with NHERF-2 appears to be the strongest, while there is no association between HPV-18 E6ΔPBM and NHERF-2. To confirm that the interaction was PDZ-PBM-mediated in each of the HPV types, the assay was repeated, including GST fusion proteins with HPV 16 and HPV-33 E6 proteins deleted for the PBM (HPV-16 E6ΔPBM and HPV-33 E6ΔPBM). The results in Figure 1B show that there is no association between NHERF-2 and HPV E6 in the absence of a functional PDZ-binding domain. These results suggest that NHERF-2 can complex with multiple HR E6 proteins and that the interactions are PDZ dependent. We then proceeded to confirm that the interactions between E6s and NHERF-2 also occur in cultured cells. HEK-293 cells were transfected with HA-tagged NHERF-2; after overnight incubation the cells were harvested and proteins extracted in E1A

buffer. The extracts were incubated with GST-16 E6, GST-18 E6, GST-11 E6, GST-33 E6, or GST alone for control. Bound proteins were detected by SDS-PAGE and Western blot and the results are shown in Figure 1B. In this setting, we observed that NHERF-2 binds with equal strength to HPV-16 E6 and HPV-18 E6, while HPV-33 E6 bound NHERF-2 somewhat weakly. No interaction was detected between the LR HPV-11 E6 and NHERF-2, which was expected, since HPV-11 E6 lacks a PBM. Further, to test whether endogenous NHERF2 interacts with E6 proteins, we performed GST pulldown assays as already described, using lysates from C33-A cells. The results in Figure 1C show that all the HR E6 oncoproteins tested bind to NHERF-2, with HPV-16 E6 being the strongest interactor, while no interaction with HPV-11 E6 was detected. Together, these results suggest that, although multiple HR E6 oncoproteins bind to NHERF-2, the principal interacting partner is likely to be HPV-16 E6.

HPV-16 E6, HPV-18 E6 and HPV-33 E6 induce NHERF-2 degradation via the proteasome in a PBM-dependent manner

After we had demonstrated that HPV-16 E6, HPV-18 E6 and HPV-33 E6 oncoproteins can interact with NHERF-2, the next obvious question was to investigate the possible consequences of the E6-NHERF-2 interactions. Since substrate degradation is a characteristic of the HPV E6-PDZ interaction (11) (29), we examined whether HPV E6 oncoproteins can likewise direct the degradation of NHERF-2. To do this, 16 E6, 18 E6, 33 E6 and 11 E6 were translated *in vitro,* and co-incubated with *in vitro*-translated NHERF-2 for 1 or 2 h at 30°C. The level of NHERF-2 protein remaining was ascertained by SDS–PAGE and autoradiography. The results in Figure 2A show that HPV-16 E6 and HPV-18 E6 were efficient in

178 inducing the degradation of NHERF-2, while HPV-33 E6 induced NHERF-2
179 degradation less efficiently and HPV-11 E6 did not induce any NHERF-2
180 degradation. The weaker (HPV-33 E6) or absent (HPV-11 E6) degradative activity is
181 consistent with their lower binding affinity or complete lack of interaction with NHERF-
182 2 respectively.
183
184 To investigate whether E6 oncoproteins can degrade NHERF-2 in cultured cells,
185 HEK-293 cells were co-transfected with a plasmid expressing HA-tagged NHERF-2
186 either alone or in combination with HPV-16 E6, HPV-18 E6, HPV-11 E6 or HPV-33
187 E6 expression plasmids, in two sets of experiments. In one set of experiments, the
188 transfected cells were left untreated, while in the other, the transfected cells were
189 treated with the proteasomal inhibitor Bortezomib (BTZ). After 24 h the cells were
190 harvested and NHERF-2 levels analyzed by immunoblotting. The Western blot
191 results, together with quantitative analysis based on band densitometry in Figure 2B
192 show that NHERF-2 protein levels are significantly reduced by more than 4 fold in
193 cells expressing HPV-16 E6, and by more than 2 fold in those expressing HPV-18 E6
194 and HPV-33 E6. This result indicates that HPV-16 E6 is the most efficient at inducing
195 NHERF-2 degradation, followed by HPV-18 E6 and HPV-33 E6. In cells expressing
196 the LR HPV-11 E6, there was no significant effect on NHERF-2 levels. Interestingly,
197 when the same transfected cells were treated with BTZ, E6-induced degradation of
198 NHERF-2 was prevented, indicating that it was proteasome-mediated.
199 To further examine the observed E6 effect on NHERF-2, we compared the
200 expression levels of NHERF-2 in HPV-negative C33-A cells, HPV-18-positive HeLa
201 cells, and HPV-16-positive CaSki and SiHa cells by performing Western blot analysis.
202 It is clearly visible in Figure 2C that endogenous NHERF-2 is abundant in C33-A

cells, while lower level was detected in HeLa cells and it was almost absent in CaSki and SiHa cells. This suggests that the protein turnover rates of endogenous NHERF-2 are increased in the presence of HPV-18 E6, and even further increased in the presence of HPV-16 E6. Furthermore, it implies that the protein turnover of NHERF-2 is more efficiently regulated by HPV-16 E6, which could be attributed to the stronger binding capacity of HPV-16 E6 for NHERF-2 as seen in Figure 1C. To additionally corroborate our initial observations shown in Figures 2A and B, where we showed that NHERF-2 is targeted for proteasome-mediated degradation by HPV-16 E6 and HPV-18 E6, we cultured the same HPV-positive and HPV-negative cell lines used in Figure 2C, in the presence or absence of the proteasomal inhibitor BTZ. After treatment, cells were harvested and the levels of NHERF-2 protein were analyzed by Western blotting. In the presence of BTZ, a sharp increase in the levels of NHERF-2 protein was observed in both HPV-16 and HPV-18-positive cell lines compared with the HPV-negative cell lines, where no such increase was observed (Figure 2D); suggesting that in HPV-positive cell lines derived from cervical tumors, NHERF-2 is a subject to proteasome-mediated degradation by E6.

Since cancer-causing HPV E6 proteins have PBMs through which they can interact with a specific panel of proteins (11); including NHERF-2, and then target them for proteasome-mediated degradation, we wondered whether PBM-PDZ interactions are required for NHERF-2 degradation. HEK-293 cells were co-transfected with a plasmid expressing HA-tagged NHERF-2 and plasmids expressing either HPV-16 E6 or HPV-18 E6, or with plasmids expressing respective mutant E6 proteins which lack PDZ binding motifs (16 E6ΔPBM or 18 E6ΔPBM) (30). Again, according to Western blot with quantitative analysis based on band densitometry, (Figure 3) shows that NHERF-2 protein levels were significantly downregulated in HEK-293 cells

expressing wild type HPV-16 E6 and HPV-18 E6, but not in those expressing the mutant HPV-16 E6ΔPBM or HPV-18 E6ΔPBM, suggesting that the E6 PBM is required for E6-proteasome-mediated degradation of NHERF-2.

HPV E6 silencing restores nuclear pool of NHERF-2

Having found that HPV E6 oncoproteins could degrade NHERF-2, we were next interested in assessing which cellular populations of NHERF-2 were being targeted, as previous studies have indicated both nuclear and cytoplasmic localization of NHERF-2 within the cell (28). In addition, NHERF-1, structurally related protein to NHERF-2, was previously reported to be detected in the cytoplasm, but absent from the nucleus in HPV-16 E6/E7-positive primary human foreskin keratinocytes (HFKs) (25). To examine this, we performed siRNA ablation of E6/E7, and also ablated E6AP expression, as an alternative means of reducing E6 expression levels (31) in HeLa and CaSki cells. After 72 h, the proteins from one set of cells were extracted with E1A buffer and NHERF-2 protein levels were analyzed by Western blotting; the levels of p53 protein were also analyzed as a control of E6/E7 silencing. The results in Figure 4A. show NHERF-2 upregulation in both HeLa and CaSki cells, upon treatment with siRNA against E6/E7 or E6AP. Simultaneously, cells were fixed and immunolabeled, and the pattern of NHERF-2 localization was monitored by confocal microscopy. Interestingly, E6/E7 downregulation induced the major recovery of NHERF-2 in the nucleus. This pattern was consistent in all HPV-positive cell lines used in the experiment (HeLa, CaSki and Siha) (Figures 4B, C and D). To further confirm this, we overexpressed HPV-16 E6 in HFKs. After 24 h, cells were fixed and immunolabeled, and the cellular localization of NHERF-2 was monitored by confocal microscopy. As indicated in Figure 4 E, cells that ectopically express 16 E6 exhibited

reduced levels of nuclear NHERF-2. Taken together, these results suggest that E6 preferentially targets the nuclear pool of NHERF-2, similarly to NHERF-1 (25).

E6 degradation of NHERF-2 regulates the expression of key cell cycle-related proteins

Cell cycle-related proteins including cyclins, such as cyclin D; cyclin-dependent kinases, such as CDK2 and CDK4; and cyclin-dependent kinase inhibitors, such as p21 and p27, enable cells to divide (32). For example, p27 is a critical cell cycle regulator, serving as an inhibitor of both CDK2 and CDK4, and its accumulation has been noted to result in cell cycle arrest at the G_1/S phase (33) (34). In addition, more recent reports indicate that NHERF-2 has an upregulatory effect on p27 and thus acts as a negative regulator of endothelial cell proliferation (28). Therefore, we asked whether the E6-induced proteasome-mediated degradation of NHERF-2 could have an influence on some of these cell cycle-related proteins, and especially on p27. Hence, we co-transfected HEK-293 cells with plasmids expressing HA-NHERF-2 and those expressing either HPV-16 or HPV-18 E6 wild type, or their respective mutated forms HPV-16 E6ΔPBM or HPV-18 E6ΔPBM. Expectedly, as shown in Figure 5A, the protein levels of both p27 and NHERF-2 increase when cells exogenously express NHERF-2 alone, but not when NHERF-2 is co-expressed with either HPV-16 E6 or HPV-18 E6 wild-types. Co-expression of either of the ΔPBM mutants had no effect on p27 or NHERF-2 levels (relative densitometries in the bottom panel of Figure 5A).

On the contrary, exogenous expression of NHERF-2 led to a decrease in cyclin D1 and CDK4 which was reversed upon co-expression of the wild-type E6, but not the ΔPBM mutants (relative densitometries in the bottom panel of Figure 5B). These data

suggest that the E6-induced degradation of NHERF-2 results in p27 downregulation and upregulation of cyclin D1 and CDK4, which may in turn influence cell proliferation.

Since NHERF-2 overexpression enhances p27 protein levels, while E6 degradation of NHERF-2 downregulates it, we wanted to investigate whether the effects of E6 on p27 are exclusively NHERF-2-dependent or if other cellular mechanisms are involved in this process. To do this, HEK-293 cells were co-transfected with plasmids expressing HA-tagged NHERF-2 and HPV-16 E6ΔPBM in the presence or absence of siRNA against NHERF-2 (siNHERF-2). After 72 h NHERF-2 and p27 levels were analyzed by Western blotting. As shown in Figure 5C, p27 levels were significantly increased (relative densitometries in the bottom panel of Figure 5C) in cells ectopically expressing NHERF-2, and remained high in cells co-expressing NHERF-2 and HPV-16 E6ΔPBM, presumably because the E6ΔPBM cannot induce NHERF-2 degradation, as shown in Figure 5A. Interestingly, when NHERF-2 was co-expressed with 16 E6ΔPBM in the presence of siNHERF-2, no significant upregulation of p27 was observed; suggesting that the downregulatory effects of E6 on p27 levels occur exclusively via NHERF-2.

To further confirm the underlying mechanisms, Hela cells were transfected with siRNA against E6/E7 and E6AP, since loss of E6AP can destabilize E6 (31); siRNA against luciferase was used as a control. After 72 h, proteins from cellular lysates were analyzed by Western blotting for NHERF-2, p27 and α-actinin. The results in Figure 5D show that ablation of E6 either by using siRNAE6/E7 or siE6AP leads to upregulation of NHERF-2 and p27. Secondly, we transfected CaSki cells with siRNA directed against E6AP and NHERF-2, in combination or separately, using siRNA against luciferase as a control. In this setting, we also analyzed the effect on p27

303 levels of a double knockdown of both E6AP and NHERF-2. After 72 h, cellular lysates
304 were analyzed by Western blotting for NHERF-2, p27, and α-actinin. The results in
305 Figure 5E confirm that downregulation of E6 (through siE6AP) leads to upregulation
306 of NHERF-2 and p27, and interestingly, in the cells that were doubly knocked down
307 for E6AP and NHERF-2, there was little or no upregulation of p27. We further
308 explored the endogenous p27 protein levels in relation to those of NHERF-2 and p53
309 in HPV-negative C33-A cells, HPV-18-positive HeLa cells, and HPV-16-positive
310 CaSki and SiHa cells by performing Western blot analysis. As shown in Figure 5F,
311 endogenous NHERF-2 protein levels are again abundant in C33-A cells compared
312 with HeLa, CaSki and SiHa cells. Interestingly, a similar trend is also observed for the
313 endogenous protein levels of both p27 and p53, where p27 and p53 protein levels
314 are abundant in C33-A cells compared with HeLa, CaSki and SiHa cells. Taken
315 together, these results additionally support the notion that the effects of E6 on p27
316 expression levels are primarily dependent on the E6/NHERF-2 interaction.
317
318 *HPV E6 increases cellular proliferative capacity by degrading NHERF-2*
319 Having shown that NHERF-2 overexpression can decrease Cyclin D1 and CDK4
320 protein levels, while increasing p27 protein levels, we questioned whether this effect
321 might affect cell proliferation; and if so, what influence E6-induced degradation of
322 NHERF-2 might also have? NHERF-2 has been reported to negatively regulate
323 endothelial cell proliferation (28), and studies suggest that p27 accumulation can
324 inhibit the cyclin D1-CDK4 complex, leading to cell cycle arrest at G_1/S (32), all of
325 which makes these questions compelling. To answer them, hence, we transfected
326 HEK-293 cells with empty vector (EV) or with vectors expressing HA-NHERF-2, HPV-
327 16 E6, HPV-18 E6, HPV-16 E6ΔPBM and HPV-18 E6ΔPBM alone or in combination

as indicated (Figure 6). Cell proliferation was then evaluated by the Uptiblue cell proliferation assay and the results are shown in Figure 6. Exogenous expression of NHERF-2 alone significantly decreases proliferation, compared with EV-transfected cells. However, proliferation significantly increased in cells co-expressing NHERF-2 with HPV-16 or HPV-18 E6 wild-type, but not with the E6 ΔPBM mutants (Figure 6A and B), indicating that the E6ΔPBM mutants were not able to target NHERF-2 like the wild type E6s, but were still able to stimulate cell proliferation via other mechanisms (35). When cells were transfected with plasmids expressing HPV-16 E6 alone, a significant increase in cell proliferation is observed compared with EV-transfected cells, while transfection with the HPV-16 E6ΔPBM mutant alone shows no significant change in cell proliferation (Figure 6A). Furthermore, in cells ectopically expressing HPV-16 E6 or HPV-16 E6ΔPBM alone, cellular proliferation was stimulated more strongly than in cells co-expressing NHERF-2 (Figure 6A), suggesting that the difference in cell proliferation maybe be due to the anti-proliferative effects of NHERF-2. To confirm this, expression of NHERF-2 was modulated in HPV-negative C33-A cells and HFK cells, HFK cells containing the HPV16 E6 genome (HFK_HPV16 E6), HPV-18-positive HeLa cells, and HPV-16-positive CaSki and SiHa cells. Each cell line was each transfected with a control siRNA (siLuc) or NHERF-2 siRNA (siNHERF-2) as indicated. After 48 h, a scratch wound was generated in the confluent cells and immediately photographed. Cells were again photographed again 24 h later and gap closure, which represents wound healing, was calculated. Figure 6C shows a representative assay, together with Western blot analysis and a histogram of the collated results of at least three assays. Compared with control siRNA (siLuc) groups, ablation of NHERF-2 using siRNA caused not only a decrease in the endogenous protein levels of NHERF-2, but also significantly increased wound

353 healing in both HPV-negative and HPV-positive cell lines thereby confirming the anti-
354 proliferative effects of NHERF-2 in these different cell lines. Taken together, these
355 data suggest that NHERF-2 downregulation can increase cell proliferation, while its
356 overexpression can decrease cell proliferation through upregulation of p27 and
357 inhibition of cyclin D1 and CDK4. Moreover, HPV E6-mediated NHERF-2 degradation
358 can lead to an increase in cellular proliferation. This is of obvious importance in
359 inducing a cellular state permissive for viral DNA replication, but can also contribute
360 to the ability of HR HPV types to cause malignancy.
361
362 **DISCUSSION**
363 Numerous studies have demonstrated that HR HPV E6 oncoproteins bind and
364 degrade various PDZ-domain containing proteins (11) and, so far, the majority of the
365 identified PDZ targets of E6 belong to the MAGUK protein family. Two of these
366 MAGUK family members, hScrib and MAGI-I, are preferentially targeted by HPV-16
367 E6 (36) and HPV-18 E6 (37), respectively. Interestingly, it has been shown that hDlg,
368 a third member of the MAGUK protein family, can be bound by E6 oncoproteins from
369 a wide range of HR HPV types, indicating the evolutionary conservation and
370 importance of proteins involved in various E6 functions (38). Furthermore, it was
371 reported that HPV-16 E6 can also bind and degrade NHERF-1, a PDZ domain-
372 containing protein and a member of the NHERF protein family. HPV-16 E6
373 degradation of NHERF-1 results in the activation of the PI3K/AKT signaling pathway,
374 which plays a crucial role in carcinogenesis (25). Most LR HPV E6 oncoproteins do
375 not have a PBM, while all of the HR types contain a Class I PBM, implying that this
376 HR hallmark plays a key feature in HPV-mediated carcinogenesis. This is further
377 supported by tissue culture and *in vivo* animal model studies, which showed that the

interactions between HPV E6 and PDZ-domain substrates play a major role in cellular transformation, in cooperation with E7, and in the induction of epithelial tumors (17) (18) (19) (12) (20). So far, however, little is known about the effect of HPV E6 oncoproteins on the PDZ-domain containing protein NHERF-2, even though NHERF-2 is structurally related to NHERF-1, which was previously characterized as a HR HPV-16 E6 oncoprotein substrate (25). We therefore, speculated that NHERF-2, which, like NHERF-1, is involved in various cellular processes such as signaling and proliferation control, is also likely to be a cellular substrate of some of the HPV E6 oncoproteins.

In this study, we report that the E6 oncoproteins of HPV-16, HPV-18 and HPV-33 can interact with NHERF-2. Our data indicate that the E6-NHERF-2 interaction is PDZ-PBM mediated and that the binding with HPV-16 E6 is the strongest, less strong with HPV-18 E6 and rather weak with HPV-33 E6, while LR 11 E6 on the other hand does not bind NHERF-2. The interactions of HPV-16, HPV-18 and HPV-33 E6 with NHERF-2 lead to its proteasome-mediated degradation both *in vitro* and *in vivo*. Of the E6 oncoproteins examined, HPV-16 E6 is the most efficient inducer of NHERF-2 degradation, while HPV-33 E6 is the least efficient, directly correlating with the intensity of their NHERF-2 binding. Previous studies have shown that NHERF-1, interacts exclusively with HPV-16 E6 (25). Interestingly, despite their structural similarities, this is not the case with NHERF-2, which can interact with multiple E6 proteins. Although these two NHERF family proteins are similar, it is likely that variations within their PDZ domains influences selection of their interacting partners (39) (40). Namely, it is well known that even a single amino acid change in the PBM of HPV E6 protein can alter the preferred target selection. In addition, it has been

shown that other amino acids upstream of the canonical PDZ recognition motif in E6 can influence the PBM-PDZ interactions and even minor changes in these amino acids can also have an effect on the strength of interaction (36) (40). All of these can explain the differences in the strength of interactions between the different E6 proteins and NHERF-2, as well as the corresponding differences in their degradative capabilities.

In agreement with the overexpression assays, NHERF-2 turnover is also regulated by E6 and the proteasome in HPV-positive cells. Although the endogenous protein levels of NHERF-2 are significantly lower in HPV-16-positive CaSki and SiHa cells than in HPV-18 positive HeLa cells, it appears that the NHERF-2 protein turnover is regulated via the proteasome in all the HPV-positive cell lines tested, since NHERF-2 levels are stabilized in the presence of proteasome inhibitors. Remarkably, however, even though the interaction between HPV-18 E6 and NHERF-2 is weaker compared to HPV-16 E6, it appears to be sufficient to induce proteasome-mediated NHERF-2 degradation. This finding is further supported by the restoration of nuclear pool of NHERF-2, following ablation of E6 in HeLa, CaSki and SiHa cells. Conversely, this is not the case in the HPV-negative C33-A cell line, where in the presence of proteasome inhibitors, there is no significant increase in the expression levels of endogenous NHERF-2; indicating the importance of NHERF-2 regulation in the HPV-life cycle and HPV-mediated malignancies.

Previous studies revealed that E6 can induce cellular proliferation by deregulating the G1/S transition, which is thought to be mainly an E7-controlled function (41). Our results provide new insights into the mechanisms used by HPV-16 E6 and HPV-18

E6 in involving p27 to induce cellular proliferation in epithelial cells. Intriguingly, NHERF-2 can behave as a tumor suppressor since it negatively regulates endothelial proliferation primarily by upregulating the protein expression of p27 (28). We present new evidence for a direct role of E6 in manipulating NHERF-2 regulation of the cell proliferation mechanism in epithelial cells, where by targeting NHERF-2, E6 downregulates p27 and increases the protein expression of cyclin D1 and CDK4, which ultimately results in increased cell proliferation. This is the first report showing an indirect effect of E6 on p27, which as a consequence, enhances cell proliferation. Previous studies have shown the importance of HPV E7 and p27 interactions for HPV-driven malignancies, indicating that HPV-16 and HPV-18 E7 proteins enhance cytoplasmic retention of p27, which results in an increased cellular proliferation; and this p27 localization to the cytoplasm was also revealed as a marker of poor prognosis for several cancer types (42)(43). Hence, it appears that HR HPV types 16 and 18 have developed two autonomous mechanisms of targeting the p27 cellular pathway. In one of them, E7 inactivates p27 by preserving it in the cytoplasm, resulting in increased cellular proliferation (42)(43), while in the other, HPV E6 targets the PDZ-domain containing protein NHERF-2 for proteasomal degradation, leading to the downregulation of p27 thereby promoting cellular proliferation. Both of these mechanisms emphasize the relevance of the p27 pathway for both HPV-life cycle and HPV-induced malignancies.

MATERIALS AND METHODS

Cell culture and transfections.

Human foreskin keratinocytes (HFKs) and HFKs containing the HPV16 genome (HFK_HPV16 E6) were cultured in Keratinocyte serum-free media (K-SFM; Gibco)

and penicillin/streptomycin. All other cells were cultured in Dulbecco's modified Eagle's medium (DMEM) with 10% fetal bovine serum (FBS) and penicillin/streptomycin (GIBCO). Cells were cultured at 37°C in an atmosphere enriched with 10% CO_2. HFKs, HFK_HPV16 E6, HEK-293 (human embryonic kidney), C33-A (Cervical carcinoma – HPV negative), HeLa (HPV-18 positive, cervical carcinoma), CaSKi (HPV-16 positive, cervical carcinoma) and SiHa (HPV-16 positive, cervical carcinoma) were transfected using calcium phosphate precipitation (44) or Lipofectamine RNAimax (Invitrogen), Lipofectamine 2000 (Invitrogen) according to the manufacturer's instructions.

Plasmids.

Wild-type hemagglutinin (HA)-tagged HPV-16 E6, HA-tagged 18 E6, HA-tagged 33 E6, HA-tagged 11 E6, HA-tagged 16 E6ΔPBM, HA-tagged 18 E6ΔPBM and HA-tagged NHERF-2, which have all been described previously (30) (45) (46) (29), were used. Glutathione S-transferase (GST) fusion proteins GST-16 E6, GST-18 E6, GST-33 E6, GST-11 E6 and GST-18 E6ΔPBM have also been previously described (31) (47) (48).

Antibodies.

The following antibodies were used: anti-NHERF-2, anti-p53 (DO-1), anti-α-actinin, anti-p21, anti-cyclin D1 and anti-CDK4, which were all purchased from Santa Cruz Biotechnology; Anti-HA-peroxidase (clone HA-7) (Sigma); β-galactosidase (LacZ) (Promega); Mouse and rabbit secondary antibodies conjugated to horseradish peroxidase (HRP) (DAKO); Rhodamine or Alexa Fluor (Invitrogen).

Inhibitors.

The following inhibitors were dissolved in DMSO and used at the indicated

concentrations: proteasome inhibitor Z-leu-leu-leu-al (CBZ (MG-132); Sigma) (50 μM) and proteasome inhibitor bortezomib (BTZ; Sigma) (10 μM). Protease inhibitors Cocktail Set I (Calbiochem) was dissolved in water.

Fusion protein purification and in vitro binding assays

Glutathione *S*-transferase (GST) fusion protein synthesis in DH5α competent *Escherichia coli* cells and protein purification were performed as previously described (49). Proteins were translated *in vitro* using a Promega TNT kit and radiolabeled with [^{35}S] cysteine or [^{35}S] methionine (Perkin Elmer). Equal amounts of *in vitro* translated proteins were added to GST fusion proteins bound to glutathione agarose (Sigma) and incubated for 1 h at 4°C. After extensive washing with phosphate-buffered saline (PBS) containing 0.25% NP-40, the bound proteins were analyzed by SDS-PAGE and autoradiography.

GST pulldowns using cellular extracts were performed by incubating GST fusion proteins immobilized on glutathione agarose with cells extracted in E1A buffer (25 mM HEPES, pH 7.0, 0.1% NP-40, 150 mM NaCl, plus protease inhibitor cocktail set I [Calbiochem]) for 1 h at 4°C on a rotating wheel. After extensive washing, the bound proteins were detected using SDS-PAGE and Western blotting.

Immunofluorescence

Cells were stained and fixed for immunofluorescence as previously described (48). In brief, HeLa, CaSki and SiHa cells were each grown overnight on glass coverslips before transfection with siRNA against luciferase, E6AP or E6/E7 as indicated for 72 h and then fixed with 4% paraformaldehyde for 10 min at room temperature followed by permeabilization in PBS containing 0.1% Triton X-100. Immunostaining was

performed by incubating the coverslips in PBS containing antibodies against p53 (Santa Cruz Biotechology) or NHERF-2 (Santa Cruz Biotechnology) as indicated overnight in a humidified chamber at 4°C. Secondary anti-rabbit or anti-mouse conjugated with alexa fluor or rhodamine was used as appropriate (Invitrogen). Nuclei were labeled with DAPI. Coverslips were slide mounted using Fluoroshield Mounting Medium with DAPI (GR271388-1, Cambridge, UK). Confocal fluorescence microscopy was performed using laser scanning microscope Leica TCS SP8 X, equipped with a HC PL APO CS2 63×/1.40 oil objective, 405 nm diode laser, an argon and a supercontinuum excitation lasers (Leica Microsystems). Images were acquired by sequential scanning with the excitation at 405 nm for DAPI, 488 nm for Alexa488 and 570 nm for Rhodamine Red. Detection ranges were 413-460 nm for DAPI, 496-559 nm for Alexa488 and 578-650 nm for Rhodamine Red.

In vitro degradation assays.

Proteins were transcribed and translated *in vitro* in rabbit reticulocyte lysate using the Promega TNT system according to the manufacturer's instructions. The HPV-16 E6, -18 E6, -33 E6, -11 E6 proteins were radiolabeled with [^{35}S]-cysteine while NHERF-2 was labeled with [^{35}S]-methionine. Degradation assays were performed as previously described (50). Briefly, radiolabeled proteins were mixed and incubated for the indicated times at 30ºC. Volumes were adjusted using water-primed lysate. The remaining NHERF-2 was analyzed by SDS-PAGE and autoradiography.

In vivo degradation assays.

Transfected or non-transfected cells seeded (3.5×10^5) on 60 mm dishes were treated with either dimethyl sulfoxide (DMSO) alone as a control or with the

proteasome inhibitors MG-132 or BTZ; both of which were dissolved in DMSO. Cells were harvested 24 h after treatment and cellular proteins extracted for analysis by Western blot.

Cell proliferation assay.

Cells were seeded into a 60 mm dish (3.5×10^5) in a total volume of 2.5 ml of cell culture medium. Cells were cultured overnight and were then transfected with either the Lipofectamine 2000 (according to the manufacturer's protocol) or calcium phosphate method (44); using a total of 1.0 μg of plasmid DNA. Cells were transfected with plasmids expressing NHERF-2, HPV-16 E6, HPV-16 E6 ΔPBM, HPV-18 E6, HPV-18 E6 ΔPBM alone or in combination as indicated in Figures and/or corresponding Figure legends. In order to monitor transfection efficiency, cells were co-transfected with β-galactosidase (LacZ) and checked by Western blot using the appropriate antibody. 16 h after transfection, media was aspirated, cells washed with sterile PBS, counted and seeded at 0.3×10^4 cells per well to a final volume of 100 μl in a 96-well plate and incubated for a further 10 h for cells to attach. Cell proliferation was monitored using the Uptiblue reagent (Interchim) as previously described (51). Uptiblue reagent (5%, v/v) was added to the culture medium and fluorescence measured (ex 540 nm/em 590 nm) on a Tecan fluorescence multi-well plate reader (Tecan Group Ltd., Männedorf, Switzerland) after 48 h. Results are expressed as a percentage of cell number of untransfected cells or that of the EV ± SEM vs. transfected cells or untransfected cells.

Wound healing/Scratch assay

A monolayer scratch/wound healing assay was employed as previously described (PMID:27483446). Briefly, C33-A, CaSki, HeLa, HFK and HFK containing the HPV 16E6 genome (HFK_HPV16 E6) cells were each transfected with a control siRNA (siLuc) or NHERF-2 siRNA (siNHERF-2) as indicated. After 48 h, a scratch wound was generated in the confluent cells with a sterile Artline p2 pipette tip (Thermo Scientific). Wounds were immediately photographed under a microscope using the Dino-Eye Digital Eye Piece Camera [AM7023(R4), IDCP B.V. Naarden – The Netherlands] that was connected to a computer and the DinoCapture 2.0: Microscope Imaging Software. After a further 24 h, the wounds were photographed again and wound closure was calculated: images were saved as TIFF and gap areas measured using the MRI Wound Healing Tool macro for ImageJ software (NIH) (http://dev.mri.cnrs.fr/projects/ imagejmacros/wiki/Wound_Healing_Tool). The cells were then harvested in RIPA lysis buffer and NHERF-2 protein levels were analyzed by Western blot. β–actin was used as a loading control.

Western blotting

Extraction of cellular proteins was performed as previously described (31). In brief, following incubation of cells with the proteasome inhibitors, cells were collected in cold phosphate buffer saline (PBS), pH 7.4 and centrifuged together with the cell culture medium at 4°C and 250 x *g* for 4 min. After two washing steps with cold PBS, cells were lysed with 100 μl of RIPA buffer (50 mM Tris-HCl, pH 8.0, 150 mM NaCl, 0.5% sodium desoxycholate, 1% Triton X-100, 0.1% sodium dodecyl sulfate (SDS)) supplemented with the protease inhibitors Cocktail Set I (Calbiochem) according to the manufacturer's instructions. The cell lysate was left on ice for 15 min, subjected to sonification (3 x 1 min) at 4°C and then cell debris was removed by centrifugation

at 16,250 x *g* at 4°C for 10 min. The protein content of the supernatant was determined according to the Bradford method using the Bio-Rad protein assay reagent (Bio-Rad).

Proteins were separated on either a 10 or 12% sodium dodecyl sulfate-polyacrylamide gel and transferred onto a nitrocellulose membrane by tank blotting. The membrane was blocked with 5% dry milk in PBS containing 0.1% Tween-20 for 1 h at room temperature and then incubated with the specific antibody, which was diluted in PBS with 0.1% Tween-20 containing 1% dry milk powder. The membrane was washed with PBS Tween-20 containing 1% skimmed milk (3 x 10 min), before being incubated with a peroxidase-coupled secondary antibody (anti-rabbit 1:1000 or anti-mouse 1:1000) for 1 h at room temperature. The membrane was washed again in PBS Tween-20 (3 x 10 min). Signals were developed, visualized and quantified using the Uvitec Cambridge – Alliance 4.7 imaging system (Cleaver Scientific, Rugby, Warwickshire, UK).

Statistical analysis

GraphPad Prism (GraphPad Inc., USA) software was used to analyze the data. All values are averages of at least 3 independent experiments made in triplicates, except when specified. Error bars shown in the figures represent standard error of the mean (SEM) and all results were expressed as arithmetic mean ± SEM. Differences between the experimental groups were analyzed using one-way ANOVA or student's t-test (two-tail, unpaired), statistical significant differences were shown as $p \leq 0.05$.

ACKNOWLEDGEMENTS

This work was supported by the Croatian Science Foundation (Grant no. 2246), ICGEB Early Career Return Grant (Grant no. CRP/16/018) and Ruđer Bošković

Institute Support Grant to VT. LB gratefully acknowledges research support from the Associazione Italiana per la Ricerca sul Cancro (Grant no. 18578). We are most grateful to Magdalena Grce for valuable comments on the manuscript.

CONFLICTS OF INTEREST

The authors declare no conflict of interest

REFERENCES

1. IARC Working Group on the Evaluation of Carcinogenic Risks to Humans. 2012. Biological agents. Volume 100 B. A review of human carcinogens. IARC Monogr Eval Carcinog Risks Hum 100:1–441.

2. Bouvard V, Baan R, Straif K, Grosse Y, Secretan B, El Ghissassi F, Benbrahim-Tallaa L, Guha N, Freeman C, Galichet L, Cogliano V, WHO International Agency for Research on Cancer Monograph Working Group. 2009. A review of human carcinogens--Part B: biological agents. Lancet Oncol 10:321–322.

3. zur Hausen H. 2002. Papillomaviruses and cancer: from basic studies to clinical application. Nat Rev Cancer 2:342–350.

4. Parkin DM, Bray F. 2006. Chapter 2: The burden of HPV-related cancers. Vaccine 24 Suppl 3:S3/11-25.

5. Tomaić V. 2016. Functional Roles of E6 and E7 Oncoproteins in HPV-Induced Malignancies at Diverse Anatomical Sites. Cancers (Basel) 8.

6. Moody CA, Laimins LA. 2010. Human papillomavirus oncoproteins: pathways to transformation. Nat Rev Cancer 10:550–560.

628 7. Mittal S, Banks L. 2017. Molecular mechanisms underlying human
629 papillomavirus E6 and E7 oncoprotein-induced cell transformation. Mutat Res Rev
630 Mutat Res 772:23–35.
631 8. Münger K, Werness BA, Dyson N, Phelps WC, Harlow E, Howley PM. 1989.
632 Complex formation of human papillomavirus E7 proteins with the retinoblastoma
633 tumor suppressor gene product. EMBO J 8:4099–4105.
634 9. Helt A-M, Galloway DA. 2003. Mechanisms by which DNA tumor virus
635 oncoproteins target the Rb family of pocket proteins. Carcinogenesis 24:159–169.
636 10. Scheffner M, Werness BA, Huibregtse JM, Levine AJ, Howley PM. 1990. The
637 E6 oncoprotein encoded by human papillomavirus types 16 and 18 promotes the
638 degradation of p53. Cell 63:1129–1136.
639 11. Thomas M, Narayan N, Pim D, Tomaić V, Massimi P, Nagasaka K, Kranjec C,
640 Gammoh N, Banks L. 2008. Human papillomaviruses, cervical cancer and cell
641 polarity. Oncogene 27:7018–7030.
642 12. Nguyen ML, Nguyen MM, Lee D, Griep AE, Lambert PF. 2003. The PDZ
643 ligand domain of the human papillomavirus type 16 E6 protein is required for E6's
644 induction of epithelial hyperplasia in vivo. J Virol 77:6957–6964.
645 13. Lee C, Laimins LA. 2004. Role of the PDZ domain-binding motif of the
646 oncoprotein E6 in the pathogenesis of human papillomavirus type 31. J Virol
647 78:12366–12377.
648 14. Nicolaides L, Davy C, Raj K, Kranjec C, Banks L, Doorbar J. 2011.
649 Stabilization of HPV16 E6 protein by PDZ proteins, and potential implications for
650 genome maintenance. Virology 414:137–145.
651 15. Delury CP, Marsh EK, James CD, Boon SS, Banks L, Knight GL, Roberts S.
652 2013. The role of protein kinase A regulation of the E6 PDZ-binding domain during

653 the differentiation-dependent life cycle of human papillomavirus type 18. J Virol
654 87:9463–9472.
655 16. Brimer N, Vande Pol SB. 2014. Papillomavirus E6 PDZ interactions can be
656 replaced by repression of p53 to promote episomal human papillomavirus genome
657 maintenance. J Virol 88:3027–3030.
658 17. Kiyono T, Hiraiwa A, Fujita M, Hayashi Y, Akiyama T, Ishibashi M. 1997.
659 Binding of high-risk human papillomavirus E6 oncoproteins to the human homologue
660 of the Drosophila discs large tumor suppressor protein. Proc Natl Acad Sci USA
661 94:11612–11616.
662 18. Riley RR, Duensing S, Brake T, Münger K, Lambert PF, Arbeit JM. 2003.
663 Dissection of human papillomavirus E6 and E7 function in transgenic mouse models
664 of cervical carcinogenesis. Cancer Res 63:4862–4871.
665 19. Watson RA, Thomas M, Banks L, Roberts S. 2003. Activity of the human
666 papillomavirus E6 PDZ-binding motif correlates with an enhanced morphological
667 transformation of immortalized human keratinocytes. J Cell Sci 116:4925–4934.
668 20. Shai A, Pitot HC, Lambert PF. 2010. E6-associated protein is required for
669 human papillomavirus type 16 E6 to cause cervical cancer in mice. Cancer Res
670 70:5064–5073.
671 21. Ganti K, Broniarczyk J, Manoubi W, Massimi P, Mittal S, Pim D, Szalmas A,
672 Thatte J, Thomas M, Tomaić V, Banks L. 2015. The Human Papillomavirus E6 PDZ
673 Binding Motif: From Life Cycle to Malignancy. Viruses 7:3530–3551.
674 22. Pim D, Bergant M, Boon SS, Ganti K, Kranjec C, Massimi P, Subbaiah VK,
675 Thomas M, Tomaić V, Banks L. 2012. Human papillomaviruses and the specificity of
676 PDZ domain targeting. FEBS J 279:3530–3537.

677 23. James CD, Roberts S. 2016. Viral Interactions with PDZ Domain-Containing
678 Proteins-An Oncogenic Trait? Pathogens 5.
679 24. Vaquero J, Nguyen Ho-Bouldoires TH, Clapéron A, Fouassier L. 2017. Role of
680 the PDZ-scaffold protein NHERF1/EBP50 in cancer biology: from signaling regulation
681 to clinical relevance. Oncogene 36:3067–3079.
682 25. Accardi R, Rubino R, Scalise M, Gheit T, Shahzad N, Thomas M, Banks L,
683 Indiveri C, Sylla BS, Cardone RA, Reshkin SJ, Tommasino M. 2011. E6 and E7 from
684 Human Papillomavirus Type 16 Cooperate To Target the PDZ Protein Na/H
685 Exchange Regulatory Factor 1. Journal of Virology 85:8208–8216.
686 26. Theisen CS, Wahl JK, Johnson KR, Wheelock MJ. 2007. NHERF links the N-
687 cadherin/catenin complex to the platelet-derived growth factor receptor to modulate
688 the actin cytoskeleton and regulate cell motility. Mol Biol Cell 18:1220–1232.
689 27. Weinman EJ, Hall RA, Friedman PA, Liu-Chen L-Y, Shenolikar S. 2006. The
690 association of NHERF adaptor proteins with g protein-coupled receptors and receptor
691 tyrosine kinases. Annu Rev Physiol 68:491–505.
692 28. Bhattacharya R, Wang E, Dutta SK, Vohra PK, E G, Prakash YS,
693 Mukhopadhyay D. 2012. NHERF-2 maintains endothelial homeostasis. Blood
694 119:4798–4806.
695 29. Tomaić V, Gardiol D, Massimi P, Ozbun M, Myers M, Banks L. 2009. Human
696 and primate tumour viruses use PDZ binding as an evolutionarily conserved
697 mechanism of targeting cell polarity regulators. Oncogene 28:1–8.
698 30. Thomas M, Dasgupta J, Zhang Y, Chen X, Banks L. 2008. Analysis of
699 specificity determinants in the interactions of different HPV E6 proteins with their PDZ
700 domain-containing substrates. Virology 376:371–378.

701 31. Tomaić V, Pim D, Banks L. 2009. The stability of the human papillomavirus E6
702 oncoprotein is E6AP dependent. Virology 393:7–10.
703 32. Satyanarayana A, Kaldis P. 2009. Mammalian cell-cycle regulation: several
704 Cdks, numerous cyclins and diverse compensatory mechanisms. Oncogene
705 28:2925–2939.
706 33. Vermeulen K, Van Bockstaele DR, Berneman ZN. 2003. The cell cycle: a
707 review of regulation, deregulation and therapeutic targets in cancer. Cell Prolif
708 36:131–149.
709 34. Rolfe M, Chiu MI, Pagano M. 1997. The ubiquitin-mediated proteolytic
710 pathway as a therapeutic area. J Mol Med 75:5–17.
711 35. DeFilippis RA, Goodwin EC, Wu L, DiMaio D. 2003. Endogenous human
712 papillomavirus E6 and E7 proteins differentially regulate proliferation, senescence,
713 and apoptosis in HeLa cervical carcinoma cells. J Virol 77:1551–1563.
714 36. Thomas M, Massimi P, Navarro C, Borg J-P, Banks L. 2005. The hScrib/Dlg
715 apico-basal control complex is differentially targeted by HPV-16 and HPV-18 E6
716 proteins. Oncogene 24:6222–6230.
717 37. Kranjec C, Massimi P, Banks L. 2014. Restoration of MAGI-1 expression in
718 human papillomavirus-positive tumor cells induces cell growth arrest and apoptosis. J
719 Virol 88:7155–7169.
720 38. Thomas M, Myers MP, Massimi P, Guarnaccia C, Banks L. 2016. Analysis of
721 Multiple HPV E6 PDZ Interactions Defines Type-Specific PDZ Fingerprints That
722 Predict Oncogenic Potential. PLOS Pathogens 12:e1005766.
723 39. Cunningham R, Biswas R, Steplock D, Shenolikar S, Weinman E. 2010. Role
724 of NHERF and scaffolding proteins in proximal tubule transport. Urol Res 38:257–
725 262.

726 40. Zhang Y, Dasgupta J, Ma RZ, Banks L, Thomas M, Chen XS. 2007. Structures
727 of a human papillomavirus (HPV) E6 polypeptide bound to MAGUK proteins:
728 mechanisms of targeting tumor suppressors by a high-risk HPV oncoprotein. J Virol
729 81:3618–3626.
730 41. Malanchi I, Caldeira S, Krützfeldt M, Giarre M, Alunni-Fabbroni M, Tommasino
731 M. 2002. Identification of a novel activity of human papillomavirus type 16 E6 protein
732 in deregulating the G1/S transition. Oncogene 21:5665–5672.
733 42. Charette ST, McCance DJ. 2007. The E7 protein from human papillomavirus
734 type 16 enhances keratinocyte migration in an Akt-dependent manner. Oncogene
735 26:7386–7390.
736 43. Yan X, Shah W, Jing L, Chen H, Wang Y. 2010. High-risk human
737 papillomavirus type 18 E7 caused p27 elevation and cytoplasmic localization. Cancer
738 Biol Ther 9:728–735.
739 44. Matlashewski G, Schneider J, Banks L, Jones N, Murray A, Crawford L. 1987.
740 Human papillomavirus type 16 DNA cooperates with activated ras in transforming
741 primary cells. EMBO J 6:1741–1746.
742 45. Lau AG, Hall RA. 2001. Oligomerization of NHERF-1 and NHERF-2 PDZ
743 domains: differential regulation by association with receptor carboxyl-termini and by
744 phosphorylation. Biochemistry 40:8572–8580.
745 46. Tomaic V, Pim D, Thomas M, Massimi P, Myers MP, Banks L. 2011.
746 Regulation of the Human Papillomavirus Type 18 E6/E6AP Ubiquitin Ligase Complex
747 by the HECT Domain-Containing Protein EDD. Journal of Virology 85:3120–3127.
748 47. Pim D, Tomaic V, Banks L. 2009. The Human Papillomavirus (HPV) E6*
749 Proteins from High-Risk, Mucosal HPVs Can Direct Degradation of Cellular Proteins
750 in the Absence of Full-Length E6 Protein. Journal of Virology 83:9863–9874.

751 48. Ganti K, Massimi P, Manzo-Merino J, Tomaić V, Pim D, Playford MP, Lizano
752 M, Roberts S, Kranjec C, Doorbar J, Banks L. 2016. Interaction of the Human
753 Papillomavirus E6 Oncoprotein with Sorting Nexin 27 Modulates Endocytic Cargo
754 Transport Pathways. PLoS Pathog 12:e1005854.
755 49. Szalmás A, Tomaić V, Basukala O, Massimi P, Mittal S, Kónya J, Banks L.
756 2017. The PTPN14 Tumor Suppressor Is a Degradation Target of Human
757 Papillomavirus E7. J Virol 91.
758 50. Thomas M, Glaunsinger B, Pim D, Javier R, Banks L. 2001. HPV E6 and
759 MAGUK protein interactions: determination of the molecular basis for specific protein
760 recognition and degradation. Oncogene 20:5431–5439.
761 51. Bennett Saidu NE, Bretagne M, Mansuet AL, Just P-A, Leroy K, Cerles O,
762 Chouzenoux S, Nicco C, Damotte D, Alifano M, Borghese B, Goldwasser F, Batteux
763 F, Alexandre J. 2018. Dimethyl fumarate is highly cytotoxic in KRAS mutated cancer
764 cells but spares non-tumorigenic cells. Oncotarget 9:9088–9099.
765

766 **FIGURE LEGENDS**

767 **Fig. 1.** HPV-16 E6, -18 E6 and -33 E6 proteins bind to NHERF-2 *in vitro* and *in vivo*.
768 A) Radiolabeled *in vitro* translated NHERF-2 was incubated with GST-16 E6, GST-
769 18 E6, GST-33 E6 and GST-18 E6ΔPBM or GST alone for control. Bound proteins
770 were assessed by autoradiography, and the input GST fusion proteins were
771 visualized with Coomassie staining (lower panel). Input NHERF-2 (20%) is shown.
772 B) The assay was repeated including GST-HPV-16 E6ΔPBM and GST-HPV-33
773 E6ΔPBM. C) HEK-293 cells were transfected with HA-tagged NHERF-2. After 24 h
774 cells were harvested and cell lysates were incubated with the indicated GST fusion
775 proteins. GST alone was included as a control. After extensive washing, bound

NHERF-2 was detected by Western blotting using the anti-HA antibody and is compared with the amount of NHERF-2 present in 10% of the input. The lower panel shows the positions of purified GST proteins used in the pull downs visualized with Coomasie staining. D) C33-A cell extracts were incubated with indicated GST fusion proteins. After extensive washing, bound NHERF-2 was detected by Western blotting using the anti-NHERF-2 antibody and is compared with the amount of NHERF-2 present in 10% of the input. The lower panel shows the positions of purified GST proteins used in the pull downs visualized with Coomasie staining.

Fig. 2. A number of HR HPV E6 proteins direct proteasome-mediated degradation of NHERF-2 *in vitro* and *in vivo*. A) NHERF-2, 16 E6, 18 E6, 33 E6 and 11 E6 were translated, and co-incubated at 30 °C for the times indicated. Residual NHERF-2 was then detected by SDS-PAGE and autoradiography. The E6 inputs are shown in the lower panel (lower band in each case - arrowed). Note the higher mobility of HPV-18 E6, in agreement with previously published data (36). B) Plasmid expressing NHERF-2 (HA- NHERF-2) was overexpressed in HEK-293 cells alone or in combination with HPV 16 E6, 18 E6, 11 E6 or 33 E6. Twenty-four hours after transfection, cells were incubated with or without the proteasome inhibitor (BTZ) for a further 10 h before harvesting. Cell lysates were prepared and analyzed by Western blotting using anti HA-antibody. β-galactosidase (LacZ) was used as an internal standard to monitor transfection efficiency and loading control. Relative densitometry for HA-NHERF-2 under various transfection conditions is shown in B (lower panel). The mean values ± standard error of 3 independent experiments is shown. *$p < 0.05$; **$p<0.01$; ns, not statistically significant. C) NHERF-2 protein levels were analyzed by Western blotting in cell lysates from C33-A (HPV negative), HeLa (HPV-18 positive),

CaSki and SiHa (both HPV-16 positive). D) The same cell lines were treated with either DMSO or BTZ for 10 h. Cell lysates were then prepared and analyzed by Western blotting using anti-NHERF-2 antibody. In both C and D, p53 was used as a control for proteasome inhibition, while β-actin was used as a loading control.

Fig. 3. HPV E6 degradation of NHERF-2 is PBM dependent. HA-tagged NHERF-2 was overexpressed in HEK-293 cells alone or in combination with HPV-16 E6 or -18 E6; or with their respective mutants 16 E6ΔPBM or 18 E6ΔPBM as indicated. As a negative control, HEK-293 cells were also transfected with the empty vector (EV). After 24 h of transfection, cells were harvested, lysates prepared and analyzed for NHERF-2 protein expression by Western blotting using anti-HA antibody. The expression of β-galactosidase (LacZ) was used as an internal standard to monitor transfection efficiency and loading (lower panel). Relative densitometry for HA-NHERF-2 under various transfection conditions is shown in the lower panel. The mean values ± standard error of 3 independent experiments is shown. *$p < 0.05$; **$p<0.01$; ns, not statistically significant.

Fig. 4. HPV-16 E6 and -18 E6 target nuclear pool of NHERF-2. A) HeLa and CaSki cells were transfected with the indicated siRNAs. After 72 h they were harvested and subjected to Western blot analysis using NHERF-2 antibody. p53 served as a control for E6/E7 and E6AP ablation. Overall protein loading was verified using anti-α-actinin antibody. B) Hela, C) CaSki and D) SiHa cells were transfected with siRNA Luciferase (siLuc), siRNA E6/E7 (siE6/E7) and siRNA E6AP (siE6AP). After 72 h the cells were fixed and stained for NHERF-2 and for p53, which served as a control for the E6/E7 and E6AP knockdown. E) HPV-16 E6 was overexpressed in HFK cells and

non-transfected cells were used a negative control. After 72 h the cells were fixed and stained for NHERF-2 and for p53, which served as a control for E6 transfection. Scale bar; B,D and D - 20 μm; E - 10 μm.

Fig. 5. HPV regulates p27 protein expression by targeting NHERF-2. A) HA-tagged NHERF-2 was overexpressed in HEK-293 cells alone or in combination with HPV 16 E6 or 18 E6; or with their respective mutants HPV- 16 E6ΔPBM or HPV-18 E6ΔPBM as indicated. As a negative control, HEK-293 cells were transfected with the EV. β-galactosidase (LacZ) was used as an internal standard to monitor transfection efficiency and γ–tubulin was used for loading control. After 24 h of transfection, cells were harvested and lysates prepared and analyzed by Western blotting for the protein expressions of p27 and NHERF-2 using anti-p27 and anti-NHERF-2 antibodies. Relative densitometries for p27 and NHERF-2 under various transfection conditions are shown in A (lower panel). B) Cell lysates from A were used to check for the protein expression levels of HA-NHERF-2, CyclinD1 and CDK4. Relative densitometries for CyclinD1 and CDK4 under various transfection conditions are shown in B (lower panel). β-galactosidase (LacZ) was used as an internal standard to monitor transfection efficiency and γ–tubulin was used for loading control. C) HEK-293 cells were co-transfected with the indicated plasmids alone or the EV or in combination with the control siRNA luciferase (siLuc) or NHERF-2 siRNA (siNHERF-2). Twenty-four hours after transfection, cells were harvested and whole cell lysates prepared and analyzed by Western blot using the various antibodies as indicated. β-galactosidase (LacZ) was used as an internal standard to monitor transfection efficiency, while β-actin was used as a loading control. Relative densitometries for p27 and HA-NHERF-2 under various transfection conditions are shown in C (lower

851 panel). One representative of at least 3 independent Western blots is shown. Data
852 are expressed as a fold change relative to γ-tubulin (A and B) or to β-actin (C). In
853 each case, the mean values ± standard error of 3 independent experiments is shown.
854 *p < 0.05; **p<0.01; ns, not statistically significant. D-E) HeLa and CaSki cells were
855 transfected with siRNA directed against luciferase (siLuc), E6/E7 (siE6/E7), E6AP
856 (siE6AP) and NHERF-2 (siNHERF-2), alone or in combination. After 72 h cells were
857 harvested and the levels of NHERF-2, p53, p27, and the α-actinin loading control
858 were detected by Western blotting. F) NHERF-2, p53 and p27 protein levels were
859 analyzed by Western blotting in cell lysates from C33-A (HPV negative), HeLa (HPV-
860 18 positive), CaSki and SiHa
861 (both HPV-16 positive). β-actin was used as a loading control and in each case, on
862 representative of at least three independent Western blots is shown.
863
864 **Fig. 6.** HPV E6 increases cellular proliferative capacity by degrading NHERF-2. A)
865 HEK-293 cells were transfected with the EV or with plasmids expressing HA-tagged
866 NHERF-2, 16 E6 and 16 E6ΔPBM, alone or in combination as indicated. B) HEK-293
867 cells were transfected with the EV or with plasmids expressing HA-tagged NHERF-2,
868 18 E6 and 18 E6ΔPBM alone or in combination as indicated. After 48 h of
869 transfection, cell proliferation was analyzed as described in the "Materials and
870 Methods" section. In all the experiments, data are expressed as a percentage
871 change relative to EV transfected cells, which was normalized to 100%. In each case,
872 the mean values ± standard error of 3 independent experiments is shown. *p < 0.05;
873 **p<0.01; ns, not statistically significant. C) Confluent cells (C33-A, CaSki, HeLa,
874 HFK and HFK containing HPV 16E6 genome (HFK_HPV16 E6) cells) were scratched
875 with a plastic pipette tip 48 h after being transfected with either siLuc or siNHERF-2.

876 C) Cells were photographed to capture gaps immediately post-scratch (0 h) and after
877 24 h. The bar chart shows percentage area of gap closure at 24 h. The same cells
878 were then harvested, lysed and NHERF-2 protein levels analyzed by Western blot.
879 β-actin was used as a loading control. Data are presented as means ±SD from three
880 independent experiments. *$p < 0.05$; **$p<0.01$ to control (siLuc).
881

Journal of Virology

JVI

Journal of Virology

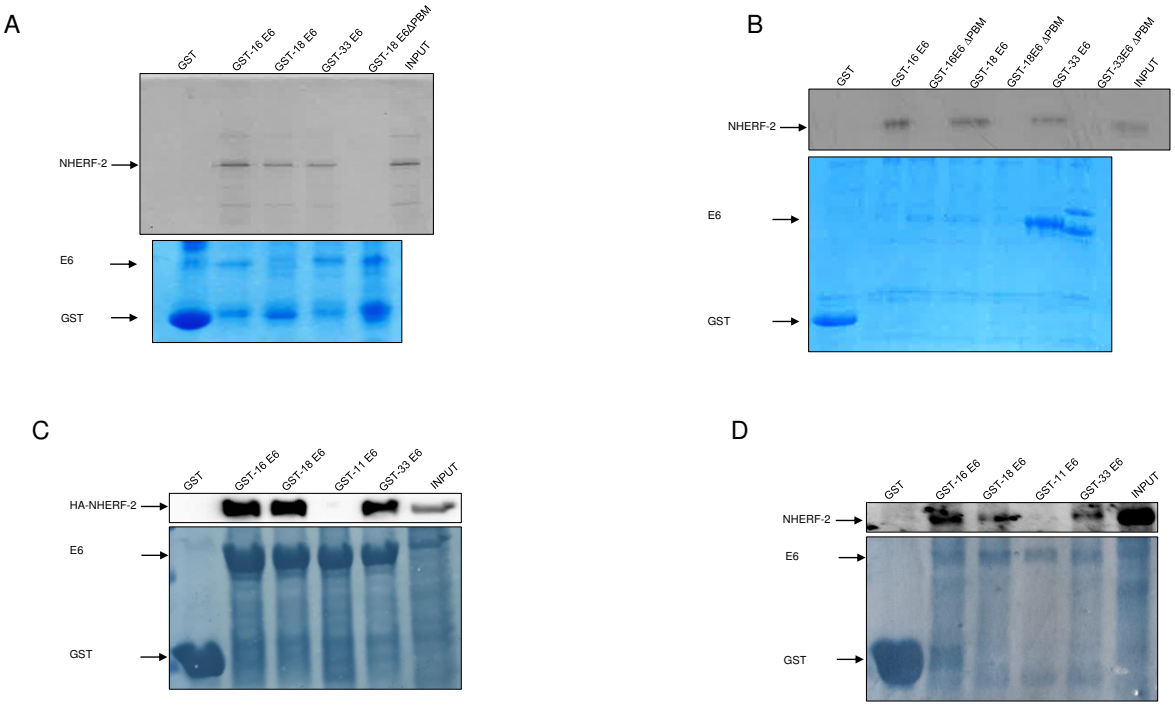

Journal of Virology

JVI

Journal of Virology

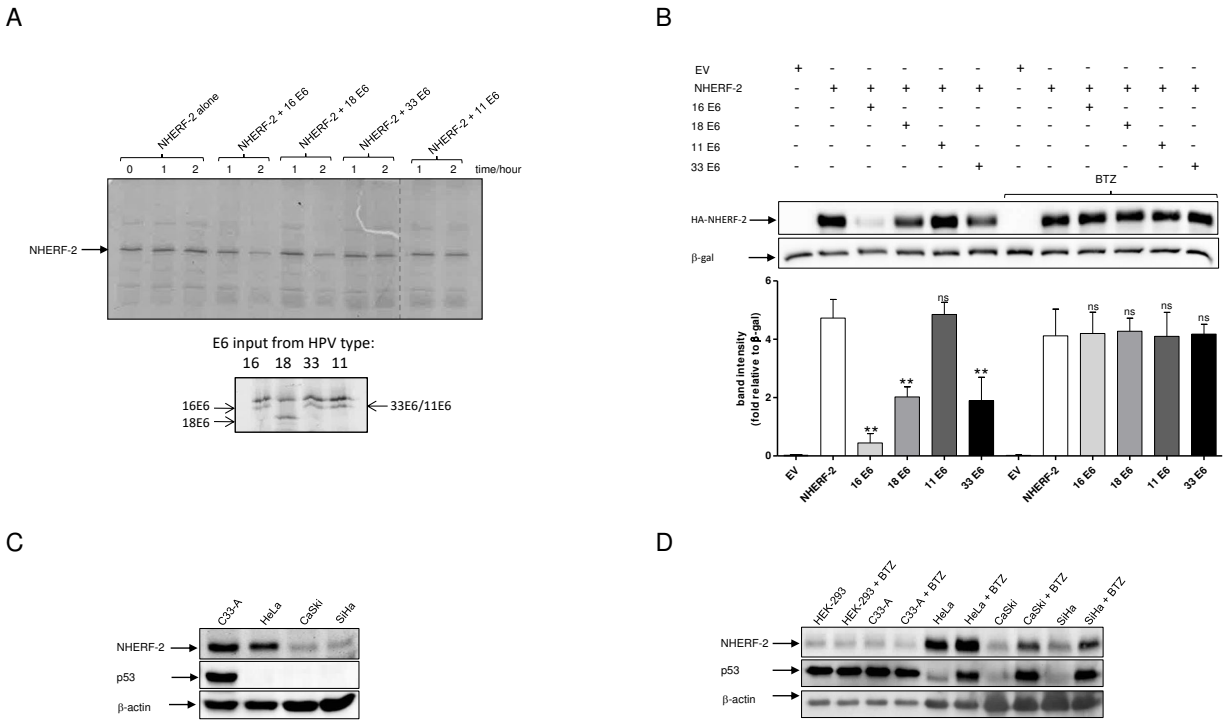

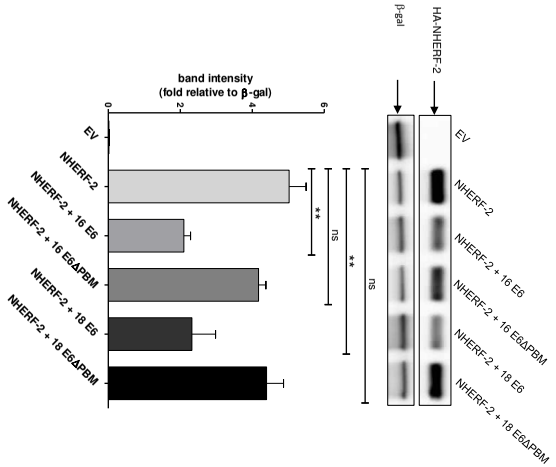

Journal of Virology

JVI

Journal of Virology

A

D

E

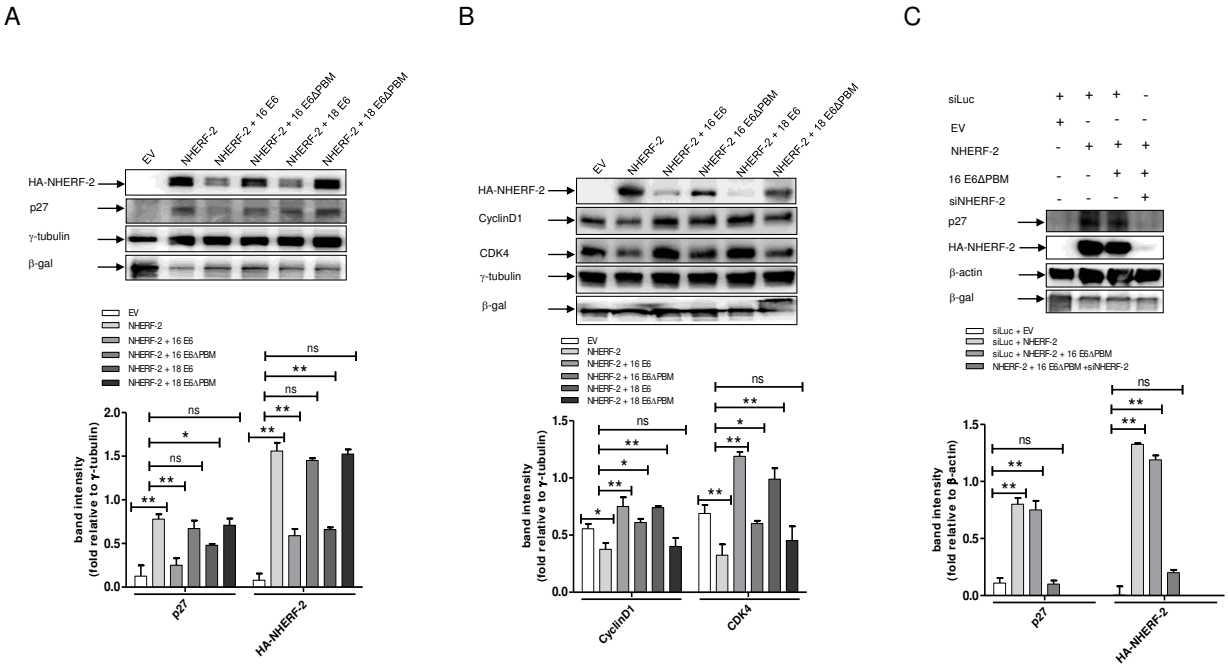

Journal of Virology

JVI

Journal of Virology

A

B

C